
Visual Correspondence Hallucination: Towards Geometric Reasoning

Hugo Germain

LIGM, École des Ponts,
Univ Gustave Eiffel, CNRS,
Marne-la-Vallée, France
hugo.germain@enpc.fr

Vincent Lepetit

LIGM, École des Ponts,
Univ Gustave Eiffel, CNRS,
Marne-la-Vallée, France
vincent.lepetit@enpc.fr

Guillaume Bourmaud

IMS, University of Bordeaux,
Bordeaux INP, CNRS,
Bordeaux, France
guillaume.bourmaud@u-bordeaux.fr

Abstract

Given a pair of partially overlapping source and target images and a keypoint in the source image, the keypoint's correspondent in the target image can be either visible, occluded or outside the field of view. Local feature matching methods are only able to identify the correspondent's location when it is visible, while humans can also hallucinate its location when it is occluded or outside the field of view through geometric reasoning. In this paper, we bridge this gap by training a network to output a peaked probability distribution over the correspondent's location, regardless of this correspondent being visible, occluded, or outside the field of view. We experimentally demonstrate that this network is indeed able to hallucinate correspondences on unseen pairs of images. We also apply this network to a camera pose estimation problem and find it is significantly more robust than state-of-the-art local feature matching-based competitors. Code will be available at hugogerman.com/neurhal.

1 Introduction

Establishing correspondences between two partially overlapping images is a fundamental computer vision problem with many applications. For example, state-of-the-art methods for visual localization from an input image rely on keypoint matches between the input image and a reference image [38, 42–44]. However, these local feature matching methods will still fail when few keypoints are *covisible*, *i.e.* when many image locations in one image are outside the field of view or become occluded in the second image.

These failures are to be expected since these methods are pure pattern recognition approaches that seek to *identify* correspondences, *i.e.* to find correspondences in covisible regions, and consider the non-covisible regions as noise. By contrast, humans explain the presence of these non-covisible regions through *geometric reasoning* and consequently are able to *hallucinate* correspondences at those locations.

Geometric reasoning has already been used in computer vision for image matching, but usually as an *a posteriori* processing [4–6, 13, 14, 21, 32]. These methods seek to remove outliers from the set of

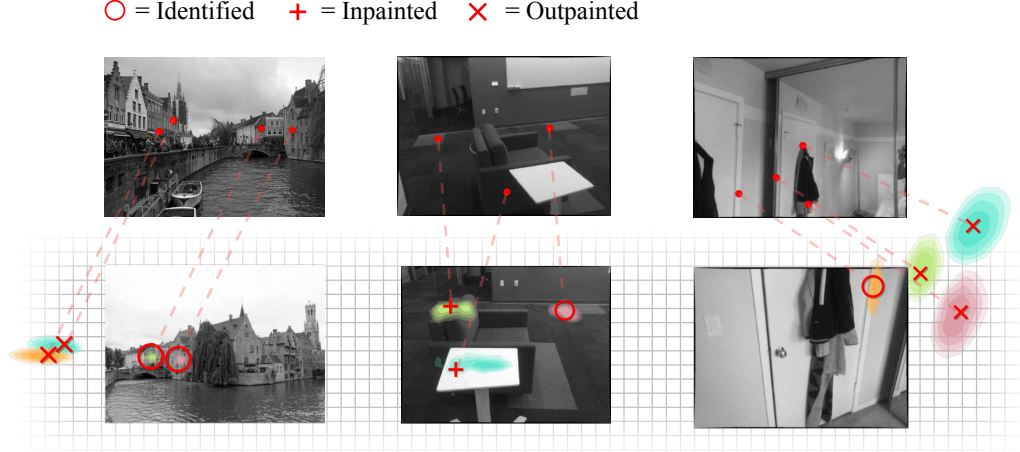


Figure 1: **Visual correspondence hallucination.** Our network, called NeurHal, takes as input a pair of partially overlapping source/target images (I_S, I_T) and keypoints $\{p_{S,n}\}_{n=1\dots N}$ in I_S , and outputs for each $p_{S,n}$ a probability distribution $C_{T,n}$ over its correspondent’s location in the image plane of I_T . When the correspondent $p_{T,n}$ of $p_{S,n}$ in I_T is visible, its location can be *identified*, whereas when $p_{T,n}$ is not visible, its location must be *hallucinated*. Two types of hallucination tasks can be distinguished: 1) if $p_{T,n}$ is occluded in I_T , its location has to be *inpainted*; 2) if $p_{T,n}$ is outside the field of view of I_T , its location needs to be *outpainted*. For each of these three pairs of source/target images coming from the test sets of ScanNet [17] and MegaDepth [28], we show (top row) I_S with a small subset of keypoints $\{p_{S,n}\}_{n=1\dots M}$ (\bullet), and (bottom row) I_T with overlaid probability distributions $\{C_{T,n}\}_{n=1\dots M}$ output by our network and the ground truth correspondents $\{p_{T,n}\}_{n=1\dots M}$ (○ for identified, + for inpainted and × for outpainted).

correspondences produced by a local feature matching approach using only limited geometric models such as epipolar geometry or planar assumptions.

While explicitly adding geometric reasoning into a neural network architecture seems difficult, we argue that learning to hallucinate correspondences in non-covisible regions could result in a network implicitly learning to perform geometric reasoning and reach human-like robustness (see Fig. 1).

Contributions. We consider a network that takes as input a pair of partially overlapping source/target images and keypoints in the source image, and outputs for each keypoint a probability distribution over its correspondent’s location in the target image plane. We propose to train this network to both identify and hallucinate the keypoints’ correspondents. We call the resulting method NeurHal, for Neural Hallucinations. To the best of our knowledge, learning to hallucinate correspondences is a virgin territory, thus we first provide an analysis of the specific features of that novel learning task. This analysis guides us towards employing an appropriate loss function and designing the architecture of the network. After training the network, we experimentally demonstrate that it is indeed able to hallucinate correspondences on unseen pairs of images. We also apply this network to a camera pose estimation problem and find it is significantly more robust than state-of-the-art local feature matching-based competitors.

2 Related work

To the best of our knowledge, aiming at hallucinating visual correspondences has never been done but the related fields of local feature description and matching are immensely vast, and we focus here only on recent learning-based approaches.

Learning-based local feature description. Using deep neural networks to learn to compute local feature descriptors have shown to bring significant improvements in invariance to viewpoint and illumination changes compared to handcrafted methods [2, 16, 22, 41]. Most methods learn

descriptors locally around pre-computed *covisible* interest regions in both images [1, 18, 31, 53], using convolutional-based siamese architectures trained with a triplet loss [3, 25, 46], contrastive loss [36] or variants [33, 47]. To further improve the performances, [20, 38] propose to jointly learn to detect and describe keypoints in both images, while [23] only detects keypoints in one image and matches against dense descriptors in the other image.

Learning-based local feature matching. All the methods described in the previous paragraph establish correspondences by comparing descriptors using a simple operation such as a dot product. Thus the combination of such a simple matching method with a siamese architecture inevitably produces outlier correspondences, especially in non-covisible regions. To reduce the amount of outliers, most approaches employ so-called Mutual Nearest Neighbor (MNN) filtering. However, it is possible to go beyond a simple MNN and learn to match descriptors. Learning-based matching methods [8, 11, 12, 34, 49, 54] take as input local descriptors and/or putative correspondences, and learn to output correspondences probabilities. However, all these matching methods focus only on predicting correctly covisible correspondences.

Jointly learning local feature description and matching. Several methods have recently proposed to jointly learn to compute and match descriptors [27, 39, 40, 43, 48]. All these methods use a siamese Convolutional Neural Network (CNN) to obtain dense local descriptors, but they significantly differ regarding the way they establish matches. They actually fall into two categories. The first category of methods [27, 39, 40] computes a 4D correlation tensor that essentially represents the scores of all the possible correspondences. This 4D correlation tensor is then used as input to a second network that learns to modify it using soft-MNN and 4D convolutions. Instead of summarizing all the information into a 4D correlation tensor, the second category of methods [43, 48] rely on so-called Transformers [10, 15, 19, 26, 37, 52, 55] to let the descriptors of both images communicate and adapt to each other. All these methods again focus on identifying correctly covisible correspondences and consider non-covisible correspondences as noise. While our architecture is closely related to the second category of methods as we also rely on Transformers, the motivation for using it is quite different since it is our goal of hallucinating correspondences that calls for a non-siamese architecture (see Sec.3).

Perhaps closest to our goal of hallucinating correspondences given a pair of partially overlapping images, is [9] that seeks to estimate a relative rotation between two non-overlapping images by learning to reason about “hidden” cues such as direction of shadows in outdoor scenes, parallel lines or vanishing points.

3 Our approach

Our goal is to train a network that takes as input a pair of partially overlapping source/target images and keypoints in the source image, and outputs for each keypoint a probability distribution over its correspondent’s location in the target image plane, regardless of this correspondent being visible, occluded, or outside the field of view. While the problem of learning to find the location of a *visible* correspondent received a lot of attention in the past few years (see Sec. 2), to the best of our knowledge, this paper is the first attempt of learning to find the location of a correspondent regardless of this correspondent being visible, occluded, or outside the field of view. Since this learning task is virgin territory, we first analyze its specific features below, before defining a loss function and a network architecture able to handle these features.

3.1 Analysis of the problem

The task of finding the location of a correspondent regardless of this correspondent being visible, occluded, or outside the field of view actually leads to three different problems. Before stating those three problems, let us first recall the notion of correspondent as it is the keystone of our problem.

Correspondent. Given a keypoint $\mathbf{p}_S \in \mathbb{R}^2$ in the source image plane, its depth $d_S \in \mathbb{R}^+$, and the relative camera pose $R_{TS} \in \text{SO}(3)$, $\mathbf{t}_{TS} \in \mathbb{R}^3$ between the coordinate systems of \mathbf{I}_S and \mathbf{I}_T , the *correspondent* $\mathbf{p}_T \in \mathbb{R}^2$ of \mathbf{p}_S in the target image plane is obtained by warping \mathbf{p}_S :

$\mathbf{p}_T := \omega(d_S, \mathbf{p}_S, \mathbf{R}_{TS}, \mathbf{t}_{TS}) := K\pi(d_S \mathbf{R}_{TS} K^{-1} \mathbf{p}_S + \mathbf{t}_{TS})$, where K is the camera calibration matrix¹ and $\pi(\mathbf{u}) := [\mathbf{u}_x/\mathbf{u}_z, \mathbf{u}_y/\mathbf{u}_z, 1]^T$ is the projection function. In a slight abuse of notation, we do not distinguish a homogeneous 2D vector from a non-homogenous 2D vector. Let us highlight that the correspondent \mathbf{p}_T of \mathbf{p}_S may not be *visible*, *i.e.* it may be occluded or outside the field of view.

Identifying the correspondent. In the case where a network has to establish a correspondence between a keypoint \mathbf{p}_S in I_S and its *visible* correspondent \mathbf{p}_T in I_T , standard approaches, such as comparing a local descriptor computed at \mathbf{p}_S in I_S with local descriptors computed at detected keypoints in I_T , are applicable to *identify* the correspondent \mathbf{p}_T .

Outpainting the correspondent. When \mathbf{p}_T is outside the field of view of I_T , there is nothing to identify, *i.e.* neither can \mathbf{p}_T be detected as a keypoint nor can a local descriptor be computed at that location. Here the network first needs to identify correspondences in the region where I_T overlaps with I_S and then perform *geometric reasoning* to realise that the correspondent \mathbf{p}_T is outside the field of view and decide to *outpaint* it (see Fig. 1). We call this operation "outpainting the correspondent" as the network needs to hallucinate the location of \mathbf{p}_T outside the field of view of I_T .

Inpainting the correspondent. When \mathbf{p}_T is occluded in I_T , the problem is even more difficult since local features can be computed at that location but will not match the local descriptor computed at \mathbf{p}_S in I_S . As in the outpainting case, the network needs to identify correspondences in the region where I_T overlaps with I_S , and finally perform *geometric reasoning* to realise that the correspondent \mathbf{p}_T is occluded and decide to *inpaint* the correspondent \mathbf{p}_T (see Fig. 1). We call this operation "inpainting the correspondent" as the network needs to hallucinate the location of \mathbf{p}_T behind the occluding object.

Let us now introduce a loss function and an architecture that are able to unify the identifying, inpainting and outpainting tasks.

3.2 Loss function

The distinction we made between the identifying, inpainting and outpainting tasks come from the fact that the source image I_S and the target image I_T are the projections of the same 3D environment from two different camera poses. In order to integrate this idea and obtain a unified correspondence learning task, we rely on the so-called *Neural Reprojection Error* (NRE) [24].

In order to properly introduce the NRE, we first recall the notion of *correspondence map*.

Correspondence map. Given I_S , I_T and a keypoint \mathbf{p}_S in the image plane of I_S , the *correspondence map* C_T of \mathbf{p}_S in the image plane of I_T is a 2D tensor of size $H_C \times W_C$ such that $C_T(\mathbf{p}_T) := p(\mathbf{p}_T | \mathbf{p}_S, I_S, I_T)$ is the likelihood of \mathbf{p}_T being the correspondent of \mathbf{p}_S . The likelihood can only be evaluated for $\mathbf{p}_T \in \Omega_{C_T}$ where Ω_{C_T} is the set of all the pixel locations in C_T . Here, we implicitly defined that the likelihood of \mathbf{p}_T falling outside the boundaries of C_T is zero. In practice, a correspondence map C_T is implemented as a neural network that takes as input \mathbf{p}_S , I_S and I_T , and outputs a softmaxed 2D tensor. A correspondence map C_T may not have the same number of lines and columns than I_T especially when the goal is to outpaint a correspondence. Thus, in the general case, to transform a 2D point from the image plane of I_T to the correspondence plane of C_T , we will need another calibration matrix K_C . Let us highlight that this likelihood is obtained using the visual information of I_S and I_T only.

Neural Reprojection Error. The NRE [24] is a loss function that warps a keypoint \mathbf{p}_S into the image plane of I_T and evaluates the negative log-likelihood at this location. In our context, the NRE can be written as:

$$\text{NRE}(\mathbf{p}_S, C_T, \mathbf{R}_{TS}, \mathbf{t}_{TS}, d_S) := -\ln C_T(\mathbf{x}_T) \text{ where } \mathbf{x}_T = K_C \omega(d_S, \mathbf{p}_S, \mathbf{R}_{TS}, \mathbf{t}_{TS}) . \quad (1)$$

In general, \mathbf{x}_T does not have integer coordinates and the notation $\ln C_T(\mathbf{x}_T)$ corresponds to performing a bilinear interpolation *after* the logarithm. For more details concerning the derivation of the NRE, the reader is referred to [24].

¹We assumed *w.l.o.g.* the source image I_S and the target image I_T are rectified images according to the pinhole camera model.

The NRE provides us with a framework to learn to identify, inpaint or outpaint the correspondent of \mathbf{p}_S in I_T in a unified manner since Eq. (1) is differentiable *w.r.t.* C_T and there is no assumption regarding covisibility. The main difficulty to overcome is the definition of a network architecture able to output a consistent C_T being given only \mathbf{p}_S , I_S and I_T as inputs, *i.e.* the network must figure out whether the correspondent of \mathbf{p}_S in I_T can be identified or has to be inpainted or outpainted.

3.3 Network architecture

The analysis from Sec. 3.1 and the use of the NRE as a loss (Sec. 3.2) call for:

- a non-siamese architecture to be able to link the information from I_S with the information from I_T to *outpaint* or *inpaint* the correspondent if needed;
- an architecture that outputs a matching score for all the possible locations in I_T as well as locations beyond the field of view of I_T as the network could decide to identify, inpaint or outpaint a correspondent at these locations.

To fulfill these requirements, we propose the following: Our network takes as input I_S and I_T as well as a set of keypoints $\{\mathbf{p}_{S,n}\}_{n=1\dots N}$ in the source image plane of I_S . A siamese CNN backbone is applied to I_S and I_T to produce compact dense local descriptor maps H_S and H_T . In order to be able to *outpaint* correspondents in the target image plane, we pad H_T with a learnable fixed vector λ . This padding step allows to *initialize* descriptors at locations outside the field of view of I_T . The amount of padding is a hyper-parameter.

The dense descriptor maps H_S and $H_{T,\text{pad}}$, and the keypoints $\{\mathbf{p}_{S,n}\}_{n=1\dots N}$ are then used as inputs of a cross-attention-based backbone \mathcal{F} with positional encoding. This part of the network outputs a feature vector $\mathbf{d}_{S,n}$ for each keypoint $\mathbf{p}_{S,n}$ and dense feature vectors $D_{T,\text{pad}}$ of the size of $H_{T,\text{pad}}$. This cross-attention-based backbone allows the local descriptors H_S and $H_{T,\text{pad}}$ to *communicate* with each other. Thus, during training, the network will be able to leverage this ability to communicate to learn to perform *geometric reasoning* and produce peaked *inpainted* and *outpainted* correspondence maps.

The correspondence map $C_{T,n}$ of $\mathbf{p}_{S,n}$ in the image plane of I_T is computed by applying a 1×1 convolution to $D_{T,\text{pad}}$ using $\mathbf{d}_{S,n}$ as filter, followed by a 2D softmax. The correspondence map $C_{T,n}$ of $\mathbf{p}_{S,n}$ in the image plane of I_T is computed by applying a 1×1 convolution to $D_{T,\text{pad}}$ using $\mathbf{d}_{S,n}$ as filter, followed by a 2D softmax.

An overview of our architecture, that we call NeurHal, is presented in Fig. 2. In practice, in order to keep the required amount of memory and the computational time reasonably low, the correspondence maps $\{C_{T,n}\}_{n=1\dots N}$ have a low resolution, *i.e.* for a target image of size 640×480 , we use a CNN with an effective stride of $s = 8$ and consequently the resulting correspondence maps (with $\gamma = 50\%$) are of size 160×120 . Producing low resolution correspondence maps prevents NeurHal from predicting accurate correspondences, but as we show in the experiments, this low resolution is sufficient to hallucinate correspondences and significantly improve the robustness of a camera pose estimator (see Sec. 4.2). We leave the question of the accuracy of hallucinated correspondences for future research. Additional details concerning the architecture are provided in the appendix.

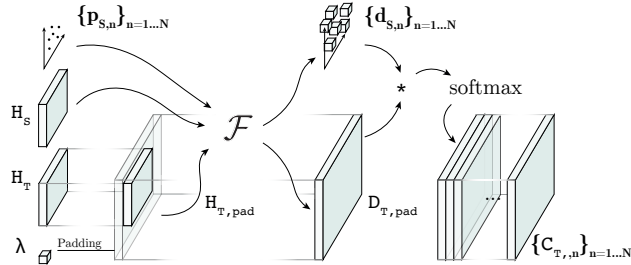


Figure 2: **Overview of NeurHal:** See text for details.

3.4 Training-time

Given a pair of partially overlapping images (I_S, I_T), a set of keypoints with ground truth depths $\{\mathbf{p}_{S,n}, d_{S,n}\}_{n=1\dots N}$ as well as the ground truth relative camera pose (R_{TS}, t_{TS}), the corresponding sum of NRE terms (Eq. 1) can be minimized *w.r.t.* the parameters of the network that produces the correspondence maps. Thus, we train our network using stochastic gradient descent and early stopping by providing pairs of overlapping images along with the aforementioned ground truth information.

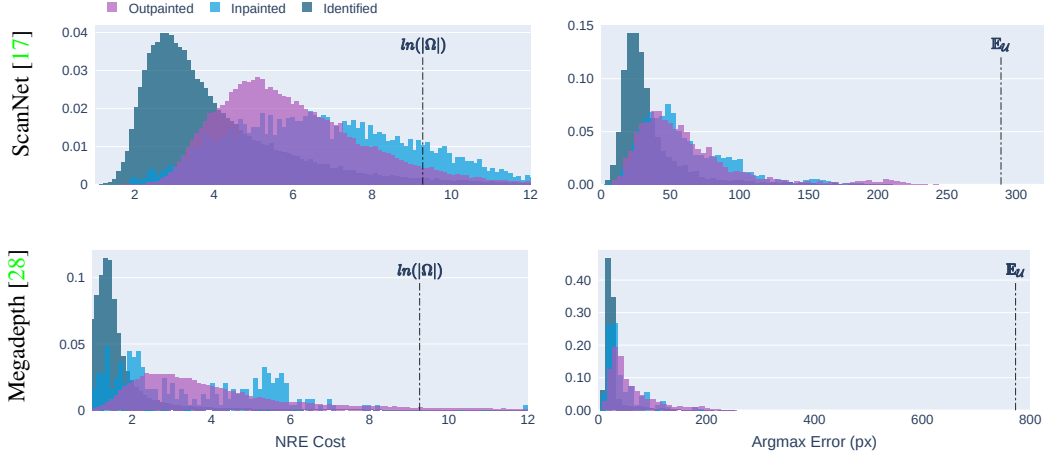


Figure 3: **Evaluation of the ability of our network to hallucinate correspondences on the test sets of ScanNet and MegaDepth.** (left) Histograms of the NRE (see Eq. 1) for each task (identifying, outpainting, inpainting), computed on correspondence maps produced by NeurHal. The value $\ln |\Omega_{C_T}|$ is the NRE of a uniform correspondence map. (right) Histograms of the errors between the argmax (mode) of a correspondence map and the ground truth correspondent’s location, for each task. The value $\mathbb{E}_{\mathcal{U}}$ is the average error of a random prediction.

Let us also highlight that there is no distinction in the training process between the identifying, inpainting and outpainting tasks since the only thing our network outputs are correspondence maps. Moreover there is no need for labeling keypoints with ground truth labels such as "identify/visible", "inpaint/occluded" or "outpaint/outside the field of view". Additional information concerning the training are provided in the appendix.

3.5 Test-time

At test-time, our network only requires a pair of partially overlapping images (I_S, I_T) as well as keypoints $\{p_{S,n}\}_{n=1\dots N}$ in I_S , and outputs a correspondence map $C_{T,n}$ in the image plane of I_T for each keypoint, regardless of its correspondent being visible, occluded or outside the field of view.

4 Experiments

In these experiments, we seek to answer two questions: 1) "Is the proposed NeurHal approach presented in Sec. 3 indeed capable of hallucinating correspondences?" and 2) "In the context of camera pose estimation, does the ability to hallucinate correspondences bring further robustness?".

4.1 Evaluation of the ability to hallucinate correspondences

We evaluate the ability of our network to hallucinate correspondences on two datasets: the indoor dataset ScanNet [17] and the outdoor dataset MegaDepth [28]. For each dataset, we train our network as described in Sec. 3.4 using the training and validation sets.

For each dataset, we run predictions over 2,500 source and target image pairs sampled from the test set, with overlaps between 2% and 80%. For every image pair, we also feed as input to NeurHal keypoints in the source image which have known ground truth correspondents in the target image and labels (visible, occluded, outside the field of view). See appendix for the computation of overlaps and labels. For this experiment, we use $\gamma = 50\%$. We then report in Fig. 3 two histograms computed over more than one million keypoints for each task we seek to validate: identification, inpainting and outpainting.

The first histogram Fig. 3 (left) is obtained by evaluating for each correspondence map the NRE cost (Eq. 1) at the ground truth correspondent’s location. In order to draw conclusions, we also report the



Figure 4: **Qualitative inpainting/outpainting results.** To illustrate the ability of NeurHal to perform visual correspondence hallucination, we display correspondence maps output by NeurHal on validation image pairs: (top row) outpainting examples, (bottom row) inpainting examples. In the source image, the red dot is a keypoint. In the target image and in the (negative log) correspondence map, the red dot represents the ground truth keypoint’s correspondent. The dashed rectangles represent the borders of the target images.

negative log-likelihood of a uniform correspondence map ($\ln |\Omega_{C_T}|$). We find that for each task and for both datasets, the predicted probability mass lies significantly below $\ln |\Omega_{C_T}|$, which demonstrates NeurHal’s ability to perform identification, inpainting and outpainting. On ScanNet [17], we also observe that identification is a simpler task than outpainting while inpainting is the hardest task. Indeed, on average the NRE cost of inpainted correspondents is higher than the average NRE cost of outpainted correspondents, which indicates the predicted correspondence maps are less peaked for inpainting than they are for outpainting. This corroborates what we empirically observed on qualitative results in Fig. 1. This finding supports our analysis Sec. 3.1. On Megadepth [28] the outpainting and inpainting histograms have a similar shape but we believe this is due to the fact that there are very few keypoints labeled as occluded in the provided SfM models (see appendix).

On the right histogram of Fig. 3, we report the distribution of the distance between the argmax of a correspondence map and the ground truth correspondent’s location. We also report the average error of a random prediction. We find the histogram mass lies significantly to the left of the random prediction average error, indicating our model is indeed able to place modes correctly in the correspondence maps, regardless of the task at hand. On ScanNet [17], we observe that the *inpainting* and *outpainting* histograms are very similar, indicating the predicted argmax is equally good for both tasks. Let us highlight that the correspondence maps produced by NeurHal have a low resolution (see Sec. 3.3) which explains why the "argmax error" is not closer to zero pixel.

These results are clear evidence that our network indeed learned to hallucinate correspondences. In Fig. 4 we show several qualitative inpainting/outpainting results.

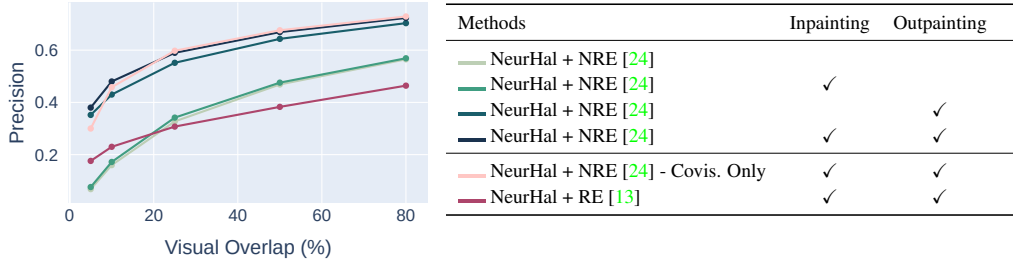


Figure 5: **Ablation study.** We compare the influence of adding inpainting and outpainting ($\gamma = 50\%$) when training NeurHal. We report the percentage of camera poses being correctly estimated for pairs of images that have an overlap between 2% and $x\%$, as a function of x , on ScanNet [17], with thresholds for translation error and rotation error of $\tau_t = 1.5m$ and $\tau_r = 20.0^\circ$. We also report results when localizing from covisible keypoints only, and using RE [13] instead of NRE [24]. Learning to hallucinate correspondences significantly improves the percentage of correctly estimated camera poses, with the outpainting learning task bringing most of the improvement.

4.2 Application to camera pose estimation

In the previous experiment we showed that our network is able to hallucinate correspondences. We now evaluate whether this ability helps improving the robustness of a camera pose estimator. We run this evaluation on the test set of ScanNet [17] over 2,500 source and target image pairs. A similar experiment on MegaDepth [28] is provided in the appendix. For each source/target image pair, we employ our network to produce correspondence maps. As in the previous experiment we use $\gamma = 50\%$. Given these correspondence maps and the depth map of the source image, we estimate the camera pose between the target image and the source image using the method proposed in [24].

In Fig. 5, we show the results of an ablation study. We focus on the robustness of the camera pose estimate, *i.e.* we consider a pose is "correct" if the rotation error is lower than 20 degrees and the translation error is below 1.5 meters. We find that training our network to perform the three tasks (identification, inpainting, and outpainting) produces the best results. We also find that using the pose estimation method proposed in [24] is very important as it allows to keep all the information of the correspondence to estimate the camera pose. This is particularly important in our context since both outpainted and inpainted correspondence maps are not very peaked (see Fig. 3&4). By comparison, a traditional pose estimator such as [13] that only keeps the argmax of the correspondences maps obtains significantly worse results. We also run an experiment where we only keep the correspondence maps of visible correspondents, *i.e.* we use ground truth labels to delete inpainted and outpainted correspondence maps before estimating the camera pose. We find that doing so only slightly decreases the performance, which shows that the identified correspondence maps benefit greatly from the geometric reasoning the network learned to perform to inpaint and outpaint correspondences during training-time.

In Fig. 6, we compare the results of our approach against state-of-the-art local feature matching methods. Fig. 6 (a) & (b) show that NeurHal is able to estimate the camera pose correctly significantly more often than any other method. Fig. 6 (c) shows that NeurHal is much more robust than state-of-the-art local feature matching methods for pairs of images with a low overlap. Fig. 6 (d) highlights the fact that when NeurHal fails to correctly estimate the camera pose, all the competitors also fail since all the methods perform similarly to the "identity" method, *i.e.* the method that consists in systematically predicting the identity pose.

5 Limitations

We identified the following limitations for our approach:

- 1 - The previous experiments showed that NeurHal is able to inpaint correspondences but the inpainted

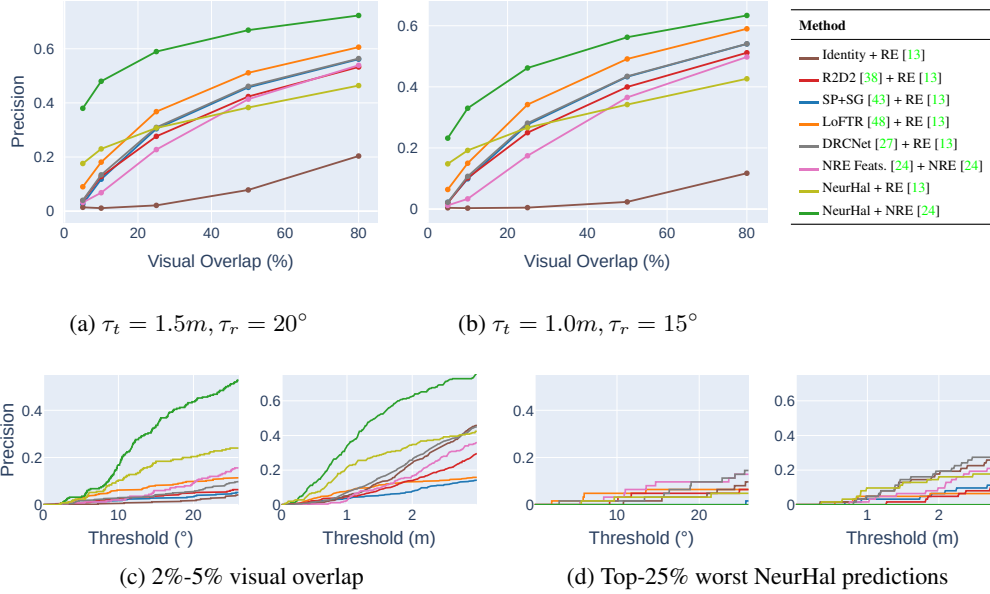


Figure 6: **Visual correspondence hallucination for camera pose estimation.** We compare the performance of NeurHal against state-of-the-art local feature matching methods on ScanNet [17]. The "identity" method consists in systematically predicting the identity pose. In (a) & (b) we report the percentage of camera poses being correctly estimated for pairs of images that have an overlap between 2% and $x\%$, as a function of x , for two rotation and translation error thresholds. In (c) we focus on image pairs with less than 5% of visual overlap. In (d) we focus on the 25% of images pairs where NeurHal has the worst camera pose estimates. See discussion at the end of Sec. 4.2.

correspondence maps are much less peaked compared to the outpainted correspondence maps. This is likely due to the fact that inpainting correspondences is much more difficult than outpainting correspondences (see Sec 3.1).

2 - The proposed architecture outputs low resolution correspondence maps (see Sec. 3.3), *e.g.* 160×120 for input images of size 640×480 and an amount of padding $\gamma = 50\%$. This is essentially due to the quadratic complexity of attention layers we use (see appendix).

3 - Our approach is able to outpaint correspondences but our correspondence maps have a finite size. Thus in the case where a keypoint's correspondent falls outside the correspondence map, the resulting correspondence map would be erroneous.

We believe these three limitations are interesting future research directions.

6 Conclusion

To the best of our knowledge, this paper is the first attempt to learn to inpaint and outpaint correspondences. We proposed an analysis of this novel learning task, which has guided us towards employing an appropriate loss function and designing the architecture of our network. We experimentally demonstrated that our network is indeed able to inpaint and outpaint correspondences on unseen images in both indoor and outdoor settings. Our results also showed that inpainting is a more challenging task than outpainting. From a practical point of view, we applied our network to a camera pose estimation problem and found that hallucinating correspondences allowed to significantly outperform the state-of-the-art feature matching methods in terms of robustness of the resulting pose estimate.

Acknowledgement

The authors would like to thank Matthieu Vilain and Rémi Giraud for their insight on visual correspondence hallucination. This project has received funding from the Bosch Research Foundation (*Bosch Forschungstiftung*). This work was granted access to the HPC resources of IDRIS under the allocation 2021-AD011011682R1 made by GENCI.

References

- [1] Vassileios Balntas, Edward Johns, Lilian Tang, and Krystian Mikolajczyk. PN-Net: Conjoined Triple Deep Network for Learning Local Image Descriptors. In *arXiv Preprint*, 2016.
- [2] Vassileios Balntas, Karel Lenc, Andrea Vedaldi, and Krystian Mikolajczyk. HPatches: A Benchmark and Evaluation of Handcrafted and Learned Local Descriptors. In *Conference on Computer Vision and Pattern Recognition*, 2017.
- [3] Vassileios Balntas, Edward Riba, Daniel Ponsa, and Krystian Mikolajczyk. Learning Local Feature Descriptors with Triplets and Shallow Convolutional Neural Networks. In *British Machine Vision Conference*, 2016.
- [4] Daniel Barath and Jiri Matas. Graph-Cut RANSAC. In *Conference on Computer Vision and Pattern Recognition*, pages 6733–6741, 2018.
- [5] Daniel Barath, Jiri Matas, and Jana Noskova. MAGSAC: Marginalizing Sample Consensus. In *Conference on Computer Vision and Pattern Recognition*, 2019.
- [6] Daniel Barath, Jana Noskova, Maksym Ivashechkin, and Jiri Matas. MAGSAC++, A Fast, Reliable and Accurate Robust Estimator. In *Conference on Computer Vision and Pattern Recognition*, pages 1301–1309, 2020.
- [7] Andrew Blake and Andrew Zisserman. *Visual Reconstruction*. MIT press, 1987.
- [8] Eric Brachmann and Carsten Rother. Neural-Guided RANSAC: Learning Where to Sample Model Hypotheses. In *International Conference on Computer Vision*, 2019.
- [9] Ruojin Cai, Bharath Hariharan, Noah Snavely, and Hadar Averbuch-Elor. Extreme Rotation Estimation using Dense Correlation Volumes. In *IEEE/CVF Conference on Computer Vision and Pattern Recognition (CVPR)*, 2021.
- [10] Mathilde Caron, Hugo Touvron, Ishan Misra, Hervé Jégou, Julien Mairal, Piotr Bojanowski, and Armand Joulin. Emerging Properties in Self-Supervised Vision Transformers. In *arXiv Preprint*, 2021.
- [11] Christopher Choy, JunYoung Gwak, Silvio Savarese, and Manmohan Chandraker. Universal Correspondence Network. In *Advances in Neural Information Processing Systems*, 2016.
- [12] Christopher Choy, Junha Lee, René Ranftl, Jaesik Park, and Vladlen Koltun. High-Dimensional Convolutional Networks for Geometric Pattern Recognition. In *Conference on Computer Vision and Pattern Recognition*, pages 11227–11236, 2020.
- [13] Ondrej Chum, Jiri Matas, and Josef Kittler. Locally Optimized RANSAC. In *DAGM Symposium on Pattern Recognition*, 2003.
- [14] Ondrej Chum, Tomas Werner, and Jiri Matas. Two-View Geometry Estimation Unaffected by a Dominant Plane. In *Conference on Computer Vision and Pattern Recognition*, pages 772–779, 2005.
- [15] Jean-Baptiste Cordonnier, Andreas Loukas, and Martin Jaggi. On the Relationship Between Self-Attention and Convolutional Layers. In *arXiv Preprint*, 2020.
- [16] Gabriela Csurka and Martin Humenberger. From Handcrafted to Deep Local Invariant Features. In *Computing Research Repository*, 2018.
- [17] Angela Dai, Angel X. Chang, Manolis Savva, Maciej Halber, Thomas Funkhouser, and Matthias Nießner. Scannet: Richly-annotated 3d reconstructions of indoor scenes. In *Proc. Computer Vision and Pattern Recognition (CVPR), IEEE*, 2017.
- [18] Daniel Detone, Tomasz Malisiewicz, and Andrew Rabinovich. SuperPoint: Self-Supervised Interest Point Detection and Description. In *Conference on Computer Vision and Pattern Recognition*, 2018.

- [19] Alexey Dosovitskiy, Lucas Beyer, Alexander Kolesnikov, Dirk Weissenborn, Xiaohua Zhai, Thomas Unterthiner, Mostafa Dehghani, Matthias Minderer, Georg Heigold, Sylvain Gelly, Jakob Uszkoreit, and Neil Houlsby. An Image Is Worth 16x16 Words: Transformers for Image Recognition at Scale. In *arXiv Preprint*, 2020.
- [20] Mihai Dusmanu, Ignacio Rocco, Tomáš Pajdla, Marc Pollefeys, Josef Sivic, Akihiko Torii, and Torsten Sattler. D2-Net: A Trainable CNN for Joint Description and Detection of Local Features. In *Conference on Computer Vision and Pattern Recognition*, 2019.
- [21] Martin A. Fischler and Robert C. Bolles. Random Sample Consensus: A Paradigm for Model Fitting with Applications to Image Analysis and Automated Cartography. In *Association for Computing Machinery*, 1981.
- [22] Steffen Gauglitz, Tobias Höllerer, and Matthew Turk. Evaluation of Interest Point Detectors and Feature Descriptors for Visual Tracking. *International Journal of Computer Vision*, 94:335–360, 2011.
- [23] Hugo Germain, Guillaume Bourmaud, and Vincent Lepetit. S2DNet: Learning Image Features for Accurate Sparse-to-Dense Matching. In *European Conference on Computer Vision*, 2020.
- [24] Hugo Germain, Vincent Lepetit, and Guillaume Bourmaud. Neural Reprojection Error: Merging Feature Learning and Camera Pose Estimation. In *Conference on Computer Vision and Pattern Recognition*, 2021.
- [25] Albert Gordo, Jon Almazán, Jérôme Revaud, and Diane Larlus. Deep Image Retrieval: Learning Global Representations for Image Search. In *European Conference on Computer Vision*, 2016.
- [26] Angelos Katharopoulos, Apoorv Vyas, Nikolaos Pappas, and Francois Fleuret. Transformers Are RNNs: Fast Autoregressive Transformers with Linear Attention. In *International Conference on Machine Learning*, 2020.
- [27] Xinghui Li, Kai Han, Shuda Li, and Victor Prisacariu. Dual-Resolution Correspondence Networks. *Advances in Neural Information Processing Systems*, 33, 2020.
- [28] Z. Li and Noah Snavely. Megadepth: Learning Single-View Depth Prediction from Internet Photos. In *Conference on Computer Vision and Pattern Recognition*, 2018.
- [29] Ilya Loshchilov and F. Hutter. Decoupled weight decay regularization. In *ICLR*, 2019.
- [30] D. G. Lowe. Distinctive Image Features from Scale-Invariant Keypoints. *International Journal of Computer Vision*, 60(2), 2004.
- [31] Zixin Luo, Tianwei Shen, Lei Zhou, Jiahui Zhang, Yao Yao, Shiwei Li, Tian Fang, and Long Quan. ContextDesc: Local Descriptor Augmentation with Cross-Modality Context. In *Conference on Computer Vision and Pattern Recognition*, pages 2522–2531, 2019.
- [32] Quan-Tuan Luong and Olivier D. Faugeras. The Fundamental Matrix: Theory, Algorithms, and Stability Analysis. *International Journal of Computer Vision*, 17(1):43–75, 1996.
- [33] Anastasiya Mishchuk, Dmytro Mishkin, Filip Radenović, and Jiri Matas. Working Hard to Know Your Neighbor’s Margins: Local Descriptor Learning Loss. In *Advances in Neural Information Processing Systems*, 2017.
- [34] Kwang Moo Yi, Eduard Trulls, Yuki Ono, Vincent Lepetit, Mathieu Salzmann, and Pascal Fua. Learning to Find Good Correspondences. In *Conference on Computer Vision and Pattern Recognition*, pages 2666–2674, 2018.
- [35] A. Paszke, S. Gross, S. Chintala, G. Chanan, E. Yang, Z. Devito, Z. Lin, A. Desmaison, L. Antiga, and A. Lerer. Automatic Differentiation in Pytorch. In *Advances in Neural Information Processing Systems*, 2017.
- [36] Filip Radenović, Giorgos Tolias, and Ondrej Chum. CNN Image Retrieval Learns from BoW: Unsupervised Fine-Tuning with Hard Examples. In *European Conference on Computer Vision*, 2016.
- [37] Prajit Ramachandran, Niki Parmar, Ashish Vaswani, Irwan Bello, Anselm Levskaya, and Jonathon Shlens. Stand-Alone Self-Attention In Vision Models. In *Advances in Neural Information Processing Systems*, 2019.
- [38] Jerome Revaud, Cesar De Souza, Martin Humenberger, and Philippe Weinzaepfel. R2D2: Reliable and Repeatable Detector and Descriptor. In *Advances in Neural Information Processing Systems*, pages 12405–12415, 2019.

- [39] Ignacio Rocco, Relja Arandjelović, and Josef Sivic. Efficient Neighbourhood Consensus Networks via Submanifold Sparse Convolutions. In *European Conference on Computer Vision*, 2020.
- [40] Ignacio Rocco, M. Cimpoi, Relja Arandjelović, Akihiko Torii, Tomás Pajdla, and Josef Sivic. Neighbourhood Consensus Networks. In *Advances in Neural Information Processing Systems*, 2018.
- [41] Ehab Salahat and Murad Qasaimeh. Recent Advances in Features Extraction and Description Algorithms: A Comprehensive Survey. In *2017 IEEE International Conference on Industrial Technology (ICIT)*, pages 1059–1063, 2017.
- [42] Paul-Edouard Sarlin, C. Cadena, R. Siegwart, and M. Dymczyk. From Coarse to Fine: Robust Hierarchical Localization at Large Scale. In *Conference on Computer Vision and Pattern Recognition*, pages 12716–12725, 2019.
- [43] Paul-Edouard Sarlin, Daniel Detone, Tomasz Malisiewicz, and Andrew Rabinovich. SuperGlue: Learning Feature Matching with Graph Neural Networks. In *Conference on Computer Vision and Pattern Recognition*, 2020.
- [44] Torsten Sattler, W. Maddern, C. Toft, Akihiko Torii, L. Hammarstrand, E. Stenborg, D. Safari, M. Okutomi, Marc Pollefeys, Josef Sivic, F. Kahl, and Tomás Pajdla. Benchmarking 6DOF Outdoor Visual Localization in Changing Conditions. In *Conference on Computer Vision and Pattern Recognition*, 2018.
- [45] J. L. Schönberger and J.-M. Frahm. Structure-From-Motion Revisited. In *Conference on Computer Vision and Pattern Recognition*, 2016.
- [46] Florian Schroff, Dmitry Kalenichenko, and James Philbin. FaceNet: A Unified Embedding for Face Recognition and Clustering. In *Computing Research Repository*, 2015.
- [47] Karen Simonyan, Andrea Vedaldi, and Andrew Zisserman. Learning Local Feature Descriptors Using Convex Optimisation. *IEEE Transactions on Pattern Analysis and Machine Intelligence*, 36, 2014.
- [48] Jiaming Sun, Zehong Shen, Yuang Wang, Hujun Bao, and Xiaowei Zhou. LoFTR: Detector-Free Local Feature Matching with Transformers. In *Conference on Computer Vision and Pattern Recognition*, 2021.
- [49] Weiwei Sun, Wei Jiang, Eduard Trulls, Andrea Tagliasacchi, and Kwang Moo Yi. ACNe: Attentive Context Normalization for Robust Permutation-Equivariant Learning. In *Conference on Computer Vision and Pattern Recognition*, pages 11286–11295, 2020.
- [50] Christian Szegedy, V. Vanhoucke, S. Ioffe, Jon Shlens, and Z. Wojna. Rethinking the Inception Architecture for Computer Vision. In *Conference on Computer Vision and Pattern Recognition*, pages 2818–2826, 2016.
- [51] Philip HS Torr and Andrew Zisserman. MLESAC: A New Robust Estimator with Application to Estimating Image Geometry. *Computer Vision and Image Understanding*, 78(1):138–156, 2000.
- [52] Ashish Vaswani, Noam M. Shazeer, Niki Parmar, Jakob Uszkoreit, Llion Jones, Aidan N. Gomez, Lukasz Kaiser, and Illia Polosukhin. Attention Is All You Need. In *arXiv Preprint*, 2017.
- [53] Kwang Moo Yi, Eduard Trulls, Vincent Lepetit, and Pascal Fua. LIFT: Learned Invariant Feature Transform. In *European Conference on Computer Vision*, 2016.
- [54] Jiahui Zhang, Dawei Sun, Zixin Luo, Anbang Yao, Lei Zhou, Tianwei Shen, Yurong Chen, Long Quan, and Hongen Liao. Learning Two-View Correspondences and Geometry Using Order-Aware Network. In *International Conference on Computer Vision*, 2019.
- [55] Hengshuang Zhao, Jiaya Jia, and Vladlen Koltun. Exploring Self-Attention for Image Recognition. In *Conference on Computer Vision and Pattern Recognition*, pages 10073–10082, 2020.

Appendix

In the following pages, we present additional experiments and technical details about our visual correspondence hallucination method NeurHal.

A Additional experiments concerning the ability to hallucinate correspondences

A.1 Additional qualitative results and failure cases

To further demonstrate the ability of NeurHal to perform visual correspondence hallucination, we report in Fig. 7 and Fig. 8 qualitative results on ScanNet [17] and Megadepth [28] respectively. In the target image and in the (negative log) correspondence map, the red dot represents the ground truth keypoint’s correspondent. The dashed rectangles represent the borders of the target images.

Let us recall that NeurHal outputs probability distributions (*a.k.a.* correspondence maps) *assuming the two inputs images are partially overlapping*. It is very important to keep this assumption in mind when looking at these qualitative results. For instance, concerning the example Fig. 7 (b) (middle), it is very difficult for our human visual system to be sure that the two images are actually overlapping, and consequently the network prediction seems to good to be true. But if we *assume* that there is an overlap, we realize that it is actually possible to perform a geometric reasoning, by drawing out the two skirting boards, to correctly outpaint the correspondent.

In fact, this overlapping assumption has a regularization effect in cases where the covisible image areas show no distinctive regions, and one image could be at an infinite translation of the other, *e.g.* Fig. 7 (b) (second to last).

In Fig. 7 (d) and Fig. 8 (d) we show failure cases where the correspondence maps modes predicted by NeurHal are either partially or completely off. We find that failure cases often correlate with strongly ambiguous image pairs, or images that have extremely limited visual overlap.

A.2 Generalization to a new domain

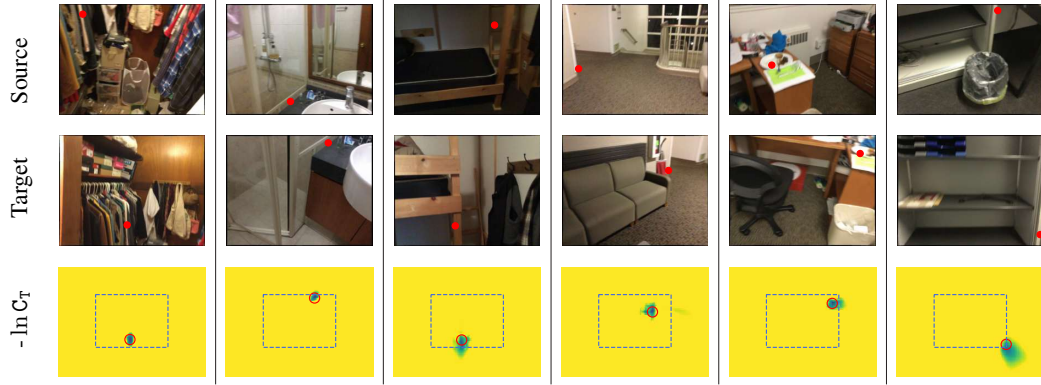
To evaluate the ability of NeurHal to perform geometric reasoning on unseen domains, we report in Fig. 9 the effect of swapping indoor and outdoor network weights, *i.e.* evaluating on ScanNet the performances of a network trained on MegaDepth, and vice versa. We find this operation has a dramatic impact on performance, strongly damaging the predicted correspondence maps. This experiment demonstrates that NeurHal is not a simple local feature matching method, but it rather performs a more intricate geometric reasoning based on the scene and its geometry.

A.3 Impact of learning to inpaint

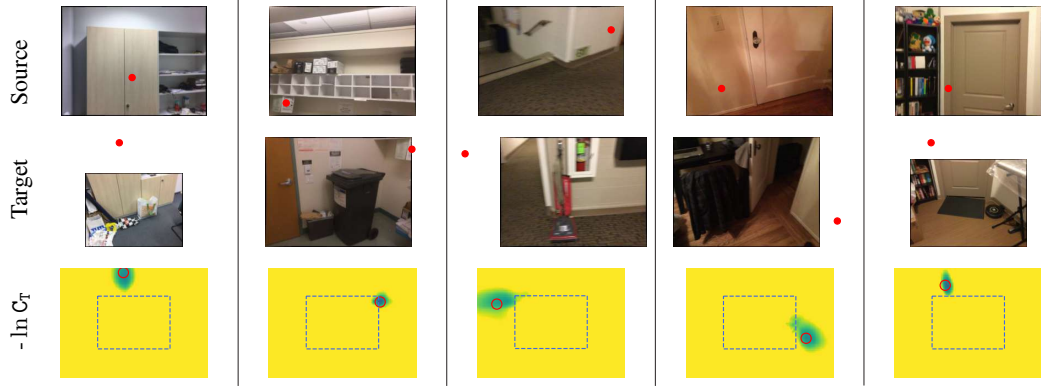
To supplement the study made in Sec. 4.1, we now aim at evaluating the impact of learning to inpaint specifically. To do so, we isolate keypoints with the *inpainted* and *outpainted* labels in our ScanNet [17] evaluation set. We then compute two sets of histograms over these keypoint subsets, one using the NRE costs evaluated at the ground truth correspondent’s locations and one using the distance in the predicted argmax location with respect to ground truth. We report in Fig. 12 the results for models trained both with and without inpainting, for $\gamma = 0\%$ and $\gamma = 50\%$.

We find that when $\gamma = 0\%$, the effect of inpainting is the most visible. We see that the histogram mass of Fig. 12 (a)(left) lies much more towards the left, which indicates correspondence maps of inpainted keypoints are more peaky when inpainting is learned. Fig. 12 (a)(right) however seems to indicate the peak of the correspondence maps of inpainted keypoints is only slightly better positioned.

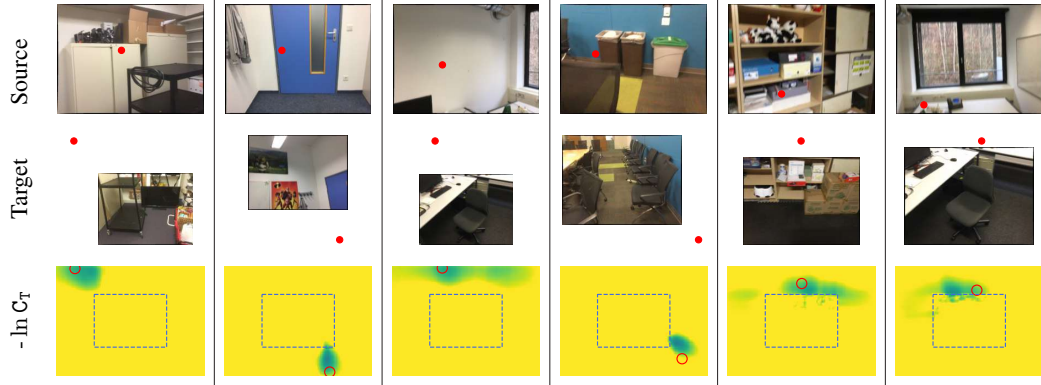
When outpainting is learned (Fig. 12 (b)), the same conclusions can be drawn with less significance. This could indicate that learning to outpaint already encourages the network to perform geometric reasoning, and that the benefit of additionally learning to inpaint keypoints is diminished.



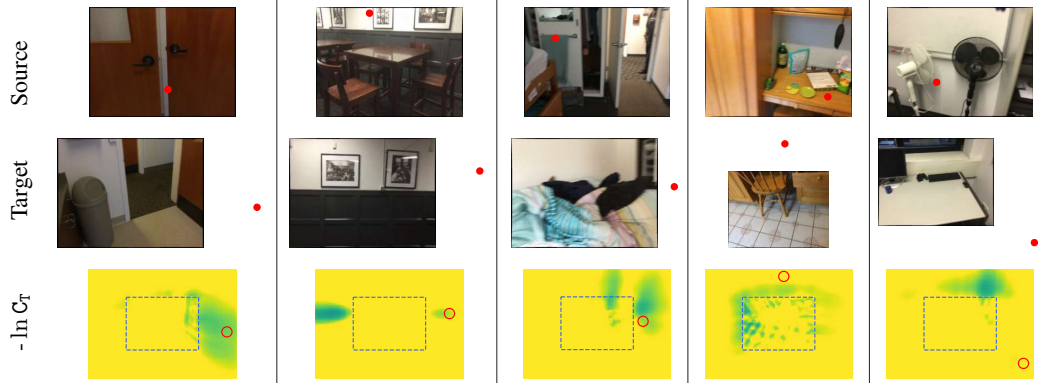
(a) Identification / Inpainting Examples



(b) Outpainting Examples

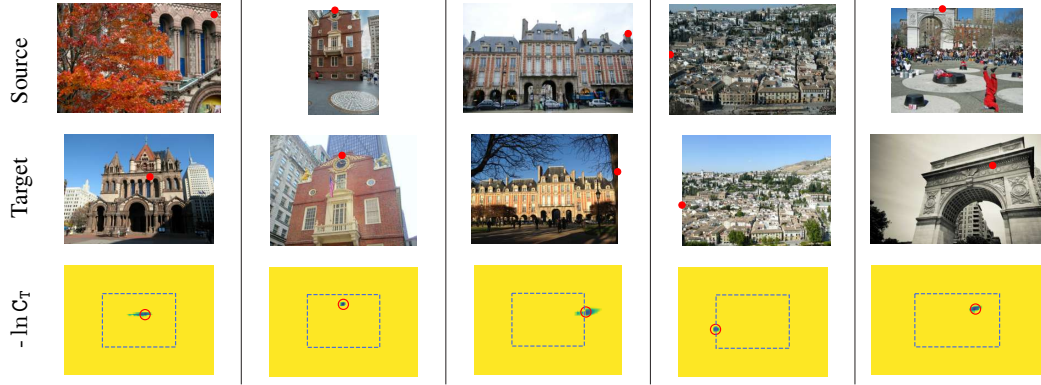


(c) Challenging Examples

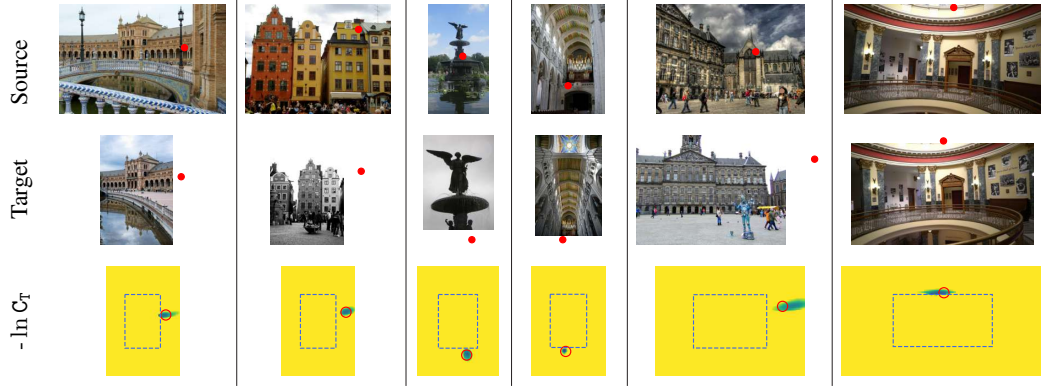


(d) Borderline / Failure Cases

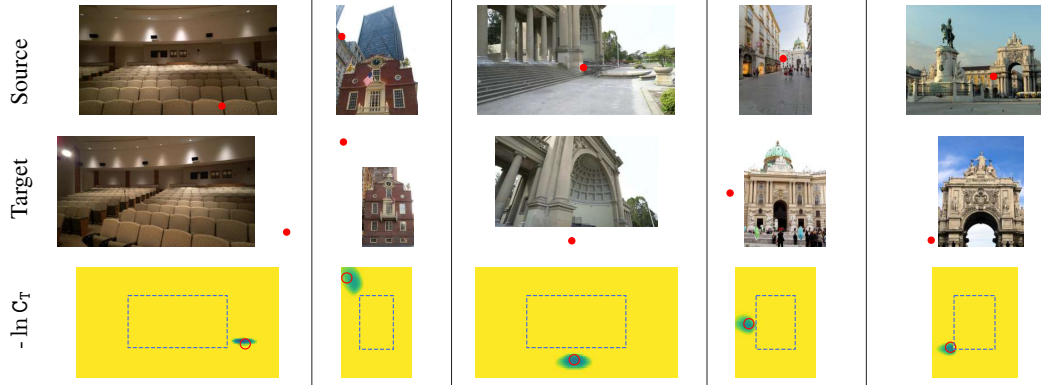
Figure 7: **Additional qualitative ScanNet [17] examples.** See text for details.



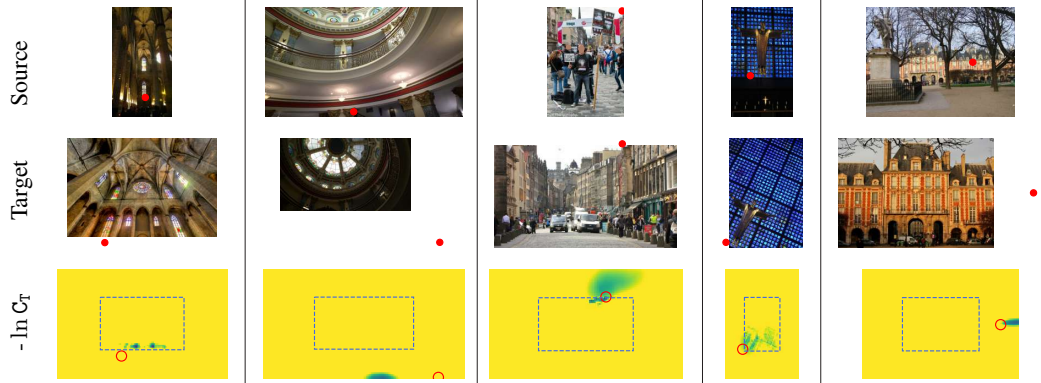
(a) Identification / Inpainting Examples



(b) Outpainting Examples



(c) Challenging Examples



(d) Borderline / Failure Cases

Figure 8: **Additional qualitative Megadepth [28] examples.** See text for details.

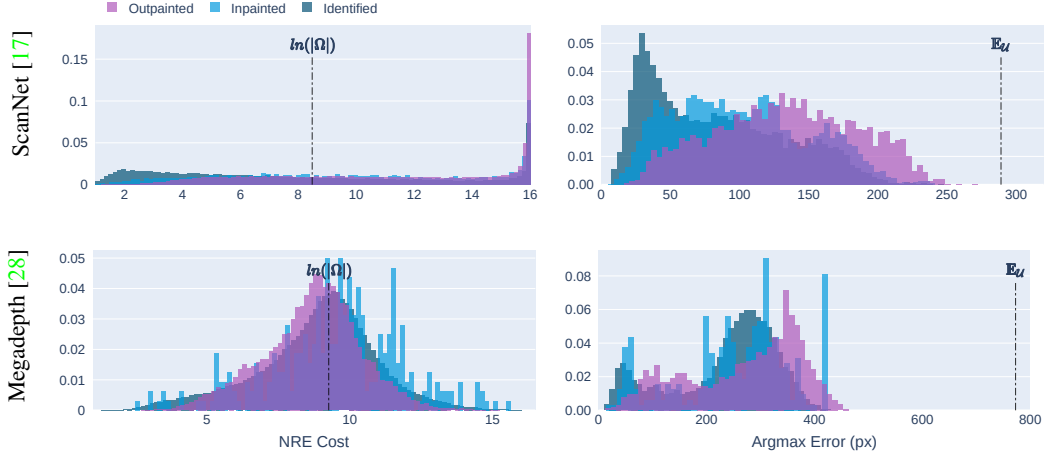


Figure 9: **Generalization to a new domain:** We evaluate the ability of NeurHal to generalize to a new domain, by evaluating on ScanNet [17] the performances of a network trained on MegaDepth [28], and vice versa. The histograms are obtained as explained in Fig. 3 of the main paper. We find that NeurHal has very little generalization capacity, which translates the fact that the model does not simply perform local feature matching, but more general geometric reasoning.

Lastly when looking at the histograms over outpainted keypoints (Fig. 12 (c)), we can see that learning to inpaint increases the peakiness of the associated correspondence maps. Here again the position of the argmax location is however only slightly impacted.

This evaluation shows that learning to inpaint is not only effective over inpainted keypoints, but it also improves the quality of the predicted correspondence maps when coupled with learning to outpaint.

B Additional experiments concerning the application to camera pose estimation

B.1 Additional qualitative results

We show in Fig. 10 qualitative results in camera pose estimation on low-overlap images from ScanNet [17], for NeurHal and its three best-performing competitors. For every method we display the keypoints used as input to the camera pose estimator in the source image, along with their reprojection at the estimated camera pose in the target image. For RE-based estimators, the keypoints are those that have been successfully matched. For NRE-based estimators, the keypoints are those involved in the prediction of the dense NRE maps. We color in keypoints based on their spatial 2D position in the source image. We find that NeurHal strongly benefits from its outpainting ability, in comparison with all other competitors which struggle to find both sufficient and reliable correspondences. We also report in Fig. 11 failure cases for NeurHal. We find that such cases correspond to image pairs exhibiting extremely limited visual overlap, strong camera pose rotations and overall significant ambiguities.

B.2 Impact of the value of γ

We report in Fig. 13 the camera pose estimation performance for varying values of γ . We compute the percentage of camera poses being correctly estimated for ScanNet [17] test images pairs that have an overlap between 2% and $x\%$ (as a function of x) for a translation threshold of $1.5m$ and a rotation threshold of 20.0° . We find that using only a small percentage of outpainting such as $\gamma = 10\%$ slightly damages the evaluation performance, which is most likely due to the small amount of added training keypoints compared to the high number of additional classes in the correspondence maps. For higher γ values however significant gains are visible, especially at small visual overlaps. This experiments demonstrates the benefit of learning to outpaint correspondences beyond image borders, and broaden the extent of usable source keypoints to perform camera pose estimation.

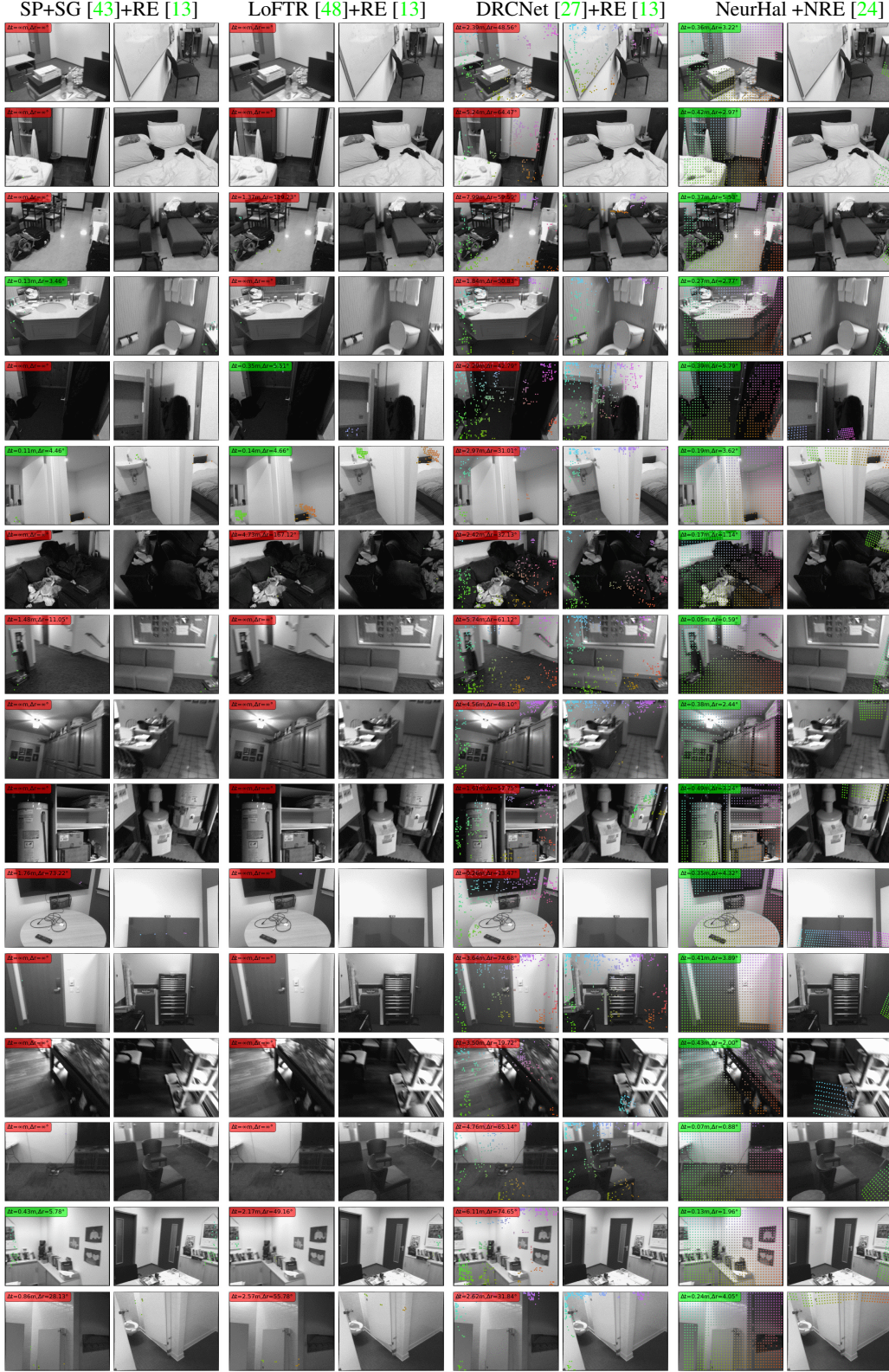


Figure 10: **Qualitative camera pose estimation results on low-overlap images from ScanNet [17]:** We show for every method keypoints used as input for the camera pose estimator in the source image (left image), along with their predicted reprojection in the target image (right image). We color-code keypoints based 2D spatial position in the source image. We also report for every pair and every method the camera pose estimation error in translation and rotation, colored in **green** when the pose is less than $\tau_t = 0.5m$ and $\tau_r = 10.0^\circ$, and in **red** otherwise.

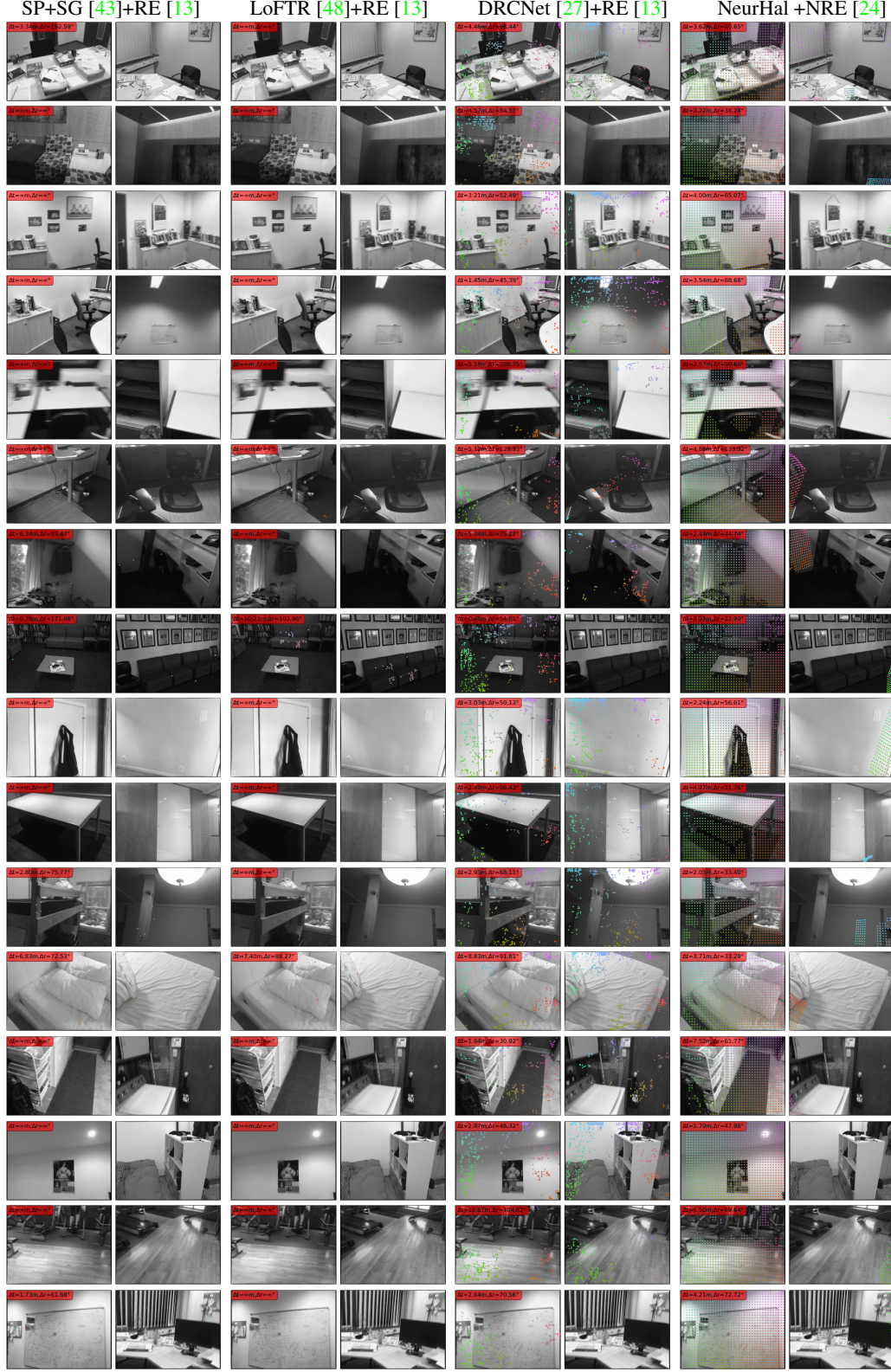


Figure 11: **NeurHal failure cases on low-overlap images from ScanNet [17]:** We report cases where NeurHal fails to estimate a camera pose with an error less than $\tau_t = 0.5m$ and $\tau_r = 10.0^\circ$. We find these cases often correlate with extremely low covisibility coupled with strong camera rotations.

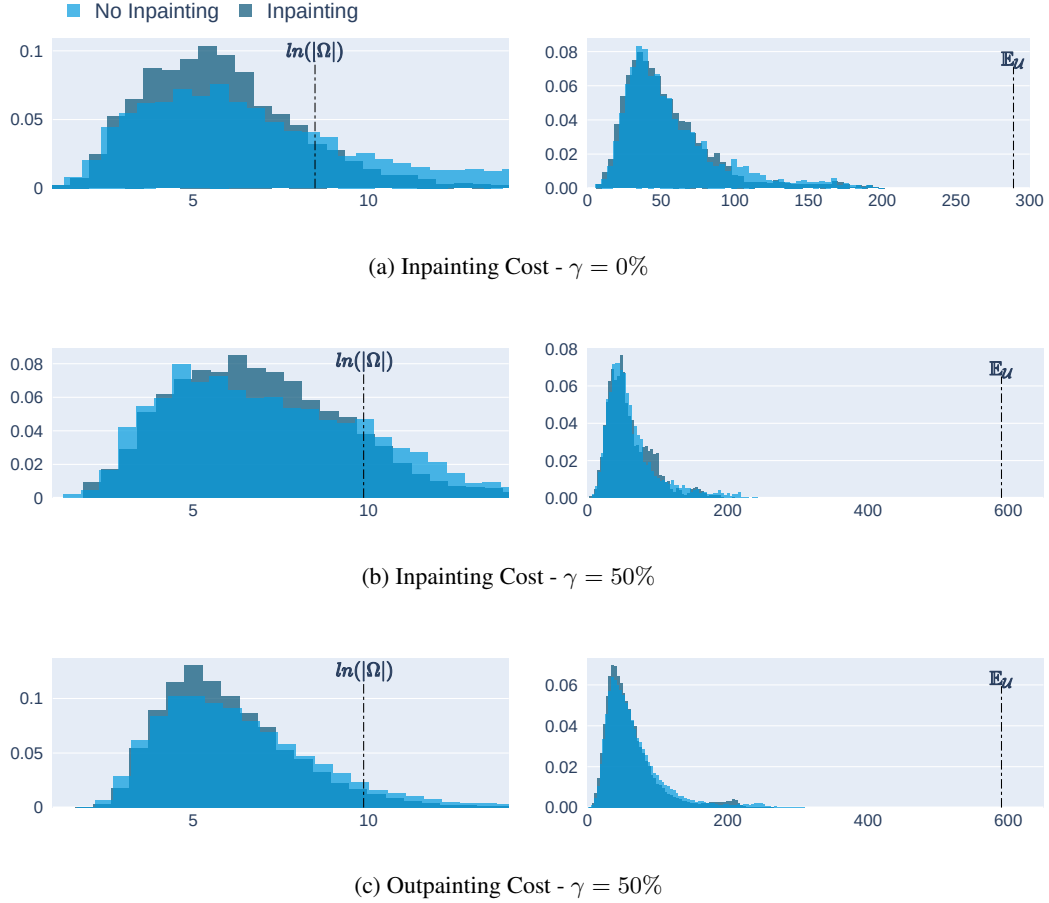


Figure 12: **Impact of learning to inpaint:** (left) Histograms of the NRE, computed on correspondence maps produced by NeurHal learned both with and without inpainting. The value $\ln |\Omega|$ is the NRE of a uniform correspondence map. (right) Histograms of the errors between the argmax (mode) of a correspondence map and the ground truth correspondent’s location, for each task. The value $\mathbb{E}_{\mathcal{U}}$ is the average error of a random prediction. We report values over inpainted keypoints ((a), (b)), as well as outpainted keypoints (c), and find that learning to inpaint is consistently beneficial to NeurHal.

B.3 Additional indoor pose estimation results

In addition to the results presented in Fig. 6 (d) of the main paper, we report in Fig. 14 the performance of NeurHal and state-of-the-art feature matching methods on ScanNet [17] image pairs with visual overlaps between 2% and 5%. For every method, we subselect the 25% of images pairs with the worst predictions, and compare it with the performance of its competitors. We find that in all cases, NeurHal strongly outperforms its competitors. On the worst NeurHal predictions, state-of-the-art methods achieve a much lower performance. For this category we can observe that all NeurHal competitors are either on par or achieve a lower performance than the Identity predictions.

B.4 Ablation study on outdoor pose estimation

To evaluate whether learning to hallucinate correspondences can bring robustness to *outdoor* camera pose estimation, we run a study similar to the one presented in Sec. 4.2 on Megadepth [28]. Megadepth consists of crowdsourced outdoor images captured in touristic places, and comes with both a sparse and dense 3D reconstruction. Please refer to Sec. C.2 for more details. Contrary to ScanNet [17], images pairs sampled from Megadepth exhibit very different geometry and relative poses. Indeed due to the nature of the photographed places, Megadepth images are often centered around the same region, and image pairs with low visual overlap are usually the result of either a strong change in

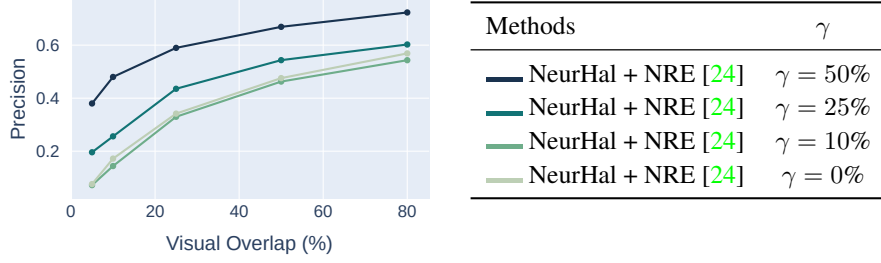


Figure 13: **Impact of the value of γ :** For increasing values of γ , we report the percentage of camera poses being correctly estimated for pairs of ScanNet [17] images that have an overlap between 2% and $x\%$ (as a function of x) for $\tau_t = 1.5m$ and $\tau_r = 20.0^\circ$. We find that a small value of $\gamma = 10\%$ yields no benefit, and even damages performance, while values of $\gamma = 25\%$ and $\gamma = 50\%$ bring significant improvements, especially at small visual overlaps.

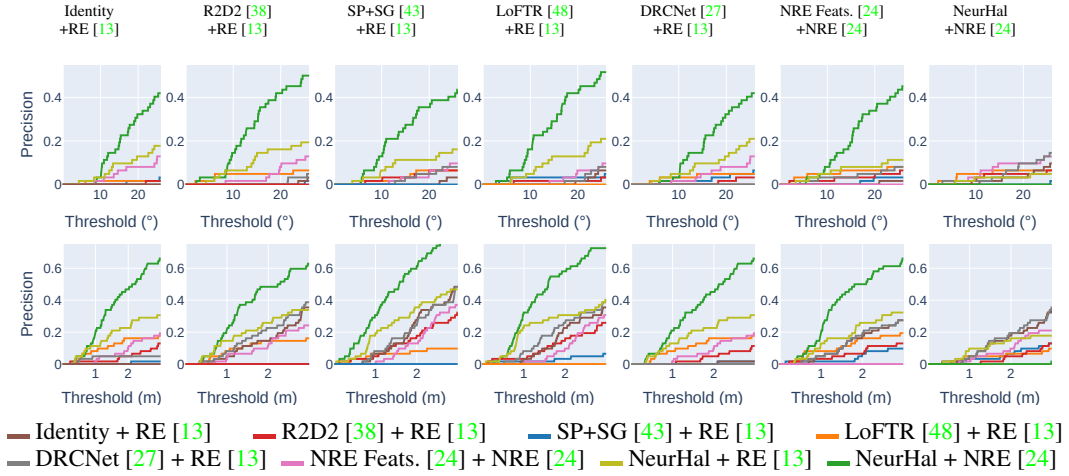


Figure 14: **Camera pose estimation experiment - Worst cases:** We report the performance of NeurHal and state-of-the-art feature matching methods on ScanNet [17] image pairs with visual overlaps between 2% and 5%. For every column, we subselect the 25% of images pairs with the worst predictions for a given method. We find that in all cases, NeurHal strongly outperforms its competitors. On the contrary, on the worst NeurHal predictions state-of-the-art methods achieve a much lower performance, on par or lower than the Identity predictions.

the focal length or a rotation around an interest region. So much so that even when learning to outpaint correspondences, a vast majority of correspondences end up outside the outpainted area on low-overlap image pairs. As a result, the ablation study results reported in Fig. 15 show that the benefits of learning to outpaint correspondences for camera pose estimation is much less visible than on ScanNet [17]. We also find that localizing on covisible keypoints only significantly improves the performance, which indicates many keypoints are reprojected in non-covisible areas which are far beyond the outpainting region.

C Technical details

C.1 Architecture details

NeurHal architecture can be separated in two building blocks: the convolutional backbone and the multi-head attention block.

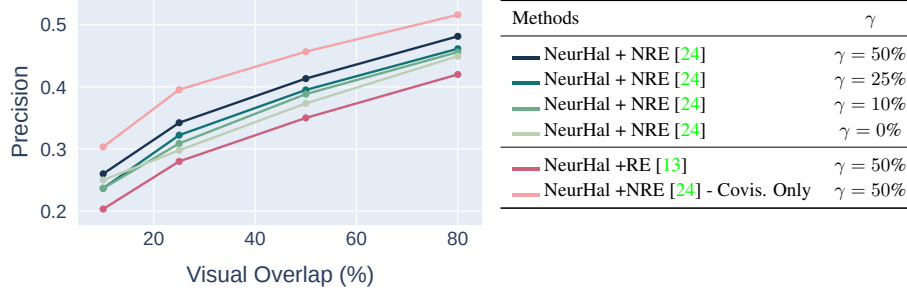


Figure 15: **Ablation study on outdoor camera pose estimation:** We compare the influence of γ in NeurHal on outdoor images. We report the percentage of camera poses being correctly estimated for pairs of images that have an overlap between 2% and $x\%$, as a function of x , on Megadepth [28], with thresholds for translation error and rotation error of $\tau_t = 5m$ and $\tau_r = 15.0^\circ$. We also report results when localizing from covisible keypoints only, and using RE [13] instead of NRE [24]. We find that contrary to ScanNet [17], the influence of γ is much more marginal. This can be attributed to the geometry of Megadepth images, as image pairs with low overlap tend to correlate with rotations around an interest regions. As such, few keypoints are outpainted and the impact of γ is less visible.

Convolutional backbone. The convolutional backbone consists of a truncated Inceptionv3 [50] model (up to Mixed-6a, 768-dimensional descriptors), modified as per NRE [24] to provide, in the case of ScanNet [17], a 1/8 output-to-input resolution ratio. To help with memory consumption we apply a simple 2D convolutional layer to compress the descriptor size to 384. In the case where $\gamma > 0$, we subsequently pad H_T with the learned vector λ , producing $H_{T, \text{pad}}$.

Positional encoding. After computing H_S and $H_{T, \text{pad}}$ with the convolutional backbone, positional encoding is applied to both dense feature maps. Similarly to SuperGlue [43], we use a 6-layer MLP of size (32, 64, 128, 256, 384), mapping a positional meshgrid between $(-1, 1)$ (centered around the image center) to higher dimensionalities. BatchNorm and ReLU layers are placed between every module. In our experiments, we tried adding more positional encoding layers but found it did not make a difference in performance. After applying the positional encoding, sparse descriptors $\{d_{s,n}\}_{n=1\dots N}$ are bilinearly interpolated at $\{p_{s,n}\}_{n=1\dots N}$ in H_S .

Self-attention. Following the positional encoding, a single multi-head attention layer is applied on $H_{T, \text{pad}}$, with 4 heads. It consists of a standard dot-product attention [52], coupled with a gating mechanism. For a given query Q , key K and value V , we compute the attention as $\text{Attention}(Q, K, V) = \text{softmax}(g * QK^T)V$ where $g = \sigma(\max(QK))$. To mitigate the quadratic cost of the dot-product attention, we also apply a max-pooling operator on keys and values with a stride of 2, as we empirically found it had very little impact on performance. We also tried using a Linear Transformer (e.g. LinFormer [26]) architecture, but despite trying numerous variants we found it consistently damaged the convergence of the model.

Cross-attention. Using the same attention-layer design, we subsequently apply it once between $\{d_{s,n}\}_{n=1\dots N}$ and H_S . This layer allows for communication between the interpolated source descriptors which will be used to produce the final correspondence maps, and the original dense source image content. Then, we apply k cross-attention layers between $\{d_{s,n}\}_{n=1\dots N}$ and $H_{T, \text{pad}}$. We empirically found these layers to be most important, as they allow for direct communication between the sparse source descriptors and the dense target feature maps, prior to the correspondence maps computation. After trying different values for k and with memory consumption in mind, we settled for $k = 4$ in all our experiments.

Layer	# of parameters
CNN	2.4 M
Positional Encoding	142 K
Self-Attention	1.9 M
Cross-Attention	7.2 M
Total	11.7 M

Table 1: **Number of parameters in NeurHal**

Implementation. The model is implemented in PyTorch [35]. For an indoor sample with 2000 keypoints it has an average throughput of 8.84 image/s on an NVIDIA RTX 3070 GPU. We report the number of parameters in our model in Table 1.

C.2 Datasets and Training details

ScanNet. The ScanNet [17] dataset is a large-scale indoor dataset containing monocular RGB videos and dense depth images, along with ground truth absolute camera poses. As SuperGlue [43] and LoFTR [48], we pre-compute visual overlaps between all image pairs for both training and test scenes. For the training set we sample images with a visual overlap between 2% and 50% from the ScanNet training scenes, which provides us with challenging images to handle. We assemble 6M image pairs, and randomly subsample 200k pairs at every training epoch. For testing images, we sample 2,500 image pairs with overlaps between 2% and 80% from the ScanNet testing scenes, using several bins to ensure sampling is close to being uniform. For both training and testing images, we sample keypoints in the source image along a regular grid with cell sizes of 16 pixels. We remove keypoints with invalid depth, as well as those where the local depth gradient is too high, as the depth information might not be reliable. We mark keypoints falling outside the target image plane as being outpainted, and we automatically detect keypoints to inpaint through a cyclic projection of the source keypoints to the target image and back. The remaining keypoints are labeled as identifiable. For all ScanNet experiments, NeurHal uses a 1/8 output-to-input resolution ratio, with a target correspondence map maximum edge size of 80 pixels (when $\gamma = 0\%$).

Megadepth. We use Megadepth [28] to train and evaluate NeurHal on outdoor images. This dataset contains over one million images captured in touristic places, and split in 196 scenes.

To train NeurHal and following the NRE [24] guidelines, we use the provided SIFT [30]-based 3D reconstruction which was made with COLMAP [45]. As for ScanNet [17] for a given image pair we consider all keypoints falling outside the target field of view as potentially outpaintable. Because the sparse 3D point cloud comes from SfM, we find however that very little keypoints can be marked as inpainted. Indeed, no 3D reconstruction is applied to objects or people occluding the scene. To allow for a wide variety of image pairs we use the sparse reconstruction to estimate the visual overlap and sample pairs with an overlap between 20% and 100%. We however find this overlap estimation to be quite unreliable, as only part of the scene is usually reconstructed.

As for ScanNet, we sample 2,500 validation image pairs with overlaps between 2% and 80%. Since Megadepth [28] images are of much higher resolution than ScanNet [17], we configure NeurHal to use a 1/16 output-to-input resolution (with a simple max-pooling layer in the CNN). We set the target correspondence map maximum edge size of 60 pixels (when $\gamma = 0\%$), to allow for space in memory when $\gamma = 50\%$.

Optimizers and scheduling. On both datasets NeurHal is trained for a maximum of 40 epochs. We use an initial learning rate of 10^{-3} , with a linear learning rate warm-up in 3 epochs from 0.1 of the initial learning rate. As [48], we decay the learning rate by 0.5 every 8 epochs starting from the 8th epoch. We apply the linear scaling rule and use a batch size of 8 over 8 NVIDIA V100 GPUs. We use the AdamW [29] optimizer, with a weight decay of 0.1. In all training procedures, we randomly initialize the model weights.

C.3 Evaluation Details

RE-based methods. For all RE [13]-based methods, we estimate the camera pose using the `pycolmap` python binding. We tune the RANSAC threshold for optimal performance, and mark all cases where less than 3 valid correspondences (*i.e.* with a valid depth value) as failure cases (infinite pose error). The remaining parameters are left as default. We follow the evaluation instructions provided by each method, and use indoor weights for SP+SG [43] and the dual-softmax indoor weights for LoFTR [48]. In the case of NeurHal +RE [13], we simply read the argmax of the predicted correspondence maps to obtain explicit 2D-to-3D correspondences.

NRE-based methods. For NRE [24]-based camera pose estimation we only use coarse models, which operate at either 1/8th or 1/16th of the original input resolution. We first retrain the NRE [24] coarse model (fully-convolutional Inceptionv3 [50], up to Mixed-6e) on the same training set as our method, with the same target resolution of 80 pixels. We refer to this model as "NRE Feats.". For both NRE Feats. and NeurHal we use the same set of regularly sampled source keypoints (see Sec. C.1), and we perform camera pose estimation first using P3P inside an MSAC [51] loop. We run P3P for a maximum of 5,000 iterations over the top-20% correspondences. We then apply a coarse GNC [7] over all source keypoints with $\sigma_{max} = 2.0$ and $\sigma_{min} = 0.6$. Let us highlight that in all the camera pose experiments, the performances of NeurHal are obtained by predicting *only* low resolution correspondence maps (see Sec. C.1).